Department of Pesticide Regulation

Brian R. Leahy
Director

M E M O R A N D U M

Edmund G. Brown Jr.
Governor

TO: Randy Segawa
Environmental Program Manager I
Environmental Monitoring Branch

FROM: Frank Spurlock, Ph.D. *Original signed by*
Research Scientist III
916-324-4124

DATE: March 20, 2013

SUBJECT: EFFECT OF CHLOROPICRIN APPLICATION PRACTICES ON CUMULATIVE AND MAXIMUM CHLOROPICRIN FLUX

INTRODUCTION

This memo summarizes modeling simulations that compare the effect of 3 types of chloropicrin application practices on cumulative flux (emission rating, ER = cumulative flux/applied fumigant) and discrete maximum 6 h period-mean flux density (ug m^{-2} s^{-1}). The practices are:

1. depth of application – 30 cm versus 45 cm application depth under bare ground, totally impermeable film (TIF) and polyethylene (PE) tarp broadcast applications;
2. effect of post-application irrigations - 0, 1,2 and 3 post-application sprinkler irrigations in bare ground broadcast applications;
3. strip versus full-field broadcast application – evaluated for TIF, PE and bare ground applications.

Chloropicrin and 1,3-dichloropropene flux data from the Lost Hills fumigation study (Ajwa and Sullivan, 2012) were used in a recent HYDRUS calibration/validation study (Spurlock et al., 2013a). That study found that the calibrated model provided estimates of ER and magnitude of peak discrete flux that were within the range of uncertainty of ISCST3 inverse-modeled flux estimates. In addition, HYDRUS also accurately simulated the individual heat transport, soil-water dynamics, fumigant partitioning and degradation processes that occurred in the field. This is important because of the potential for complex nonlinear models (such as HYDRUS) to yield desirable results, even when individual processes may not be accurately described (Hornberger and Spear, 1981). If individual processes are not accurately described, serious errors may occur when extrapolating model results to new situations. The simulations here were performed using HYDRUS, and based on the Lost Hills field 1 calibrated HYDRUS scenario where possible, including soil properties, degradation half-life and TIF tarp permeability.

SCENARIOS, MODELING PROCEDURES AND INPUT DATA

Where possible, all simulations here used measured or calibrated data from the Lost Hills studies (Spurlock et al., 2013a). Measured data included initial soil-water contents, soil bulk density, soil organic carbon, and van Genuchten soil hydraulic parameters (van Genuchten, 1980). The latter

hydraulic parameters were derived from laboratory measured soil-water retention data (Appendix 1). Spurlock et al. (2013a) used Lost Hills field 1 data to calibrate chloropicrin site-specific degradation rate, soil sorption coefficient, and the chloropicrin-TIF boundary layer depth. The boundary layer depth is the modeling parameter that describes effective TIF permeability (Table 1). Additional chloropicrin physicochemical properties and associated data sources are given in Appendix 1.

Table 1. HYDRUS calibration results for Lost Hills field 1 chloropicrin data: optimized variables and 95% CI (Spurlock et al., 2013a).

variable	chloropicrin
k_1 (d^{-1}) – first order degradation rate constant	0.1595 [A] (0.1413, 0.1777)
K_{OC} (ml g^{-1}) – sorption coefficient	66 [B]
d (cm) – TIF boundary layer depth	2230 [C] (1925, 2534)

[A] corresponds to 4.3 day half-life

[B] confidence intervals not determined

[C] corresponds to tarp mass transfer coefficient (MTC) of 0.12 cm h^{-1}

Chloropicrin-PE tarp mass transfer coefficients (MTC) Thirty-seven chloropicrin-PE tarp laboratory MTC measurements were compiled from Paperniek et al. (2011, 31 data), Paperniek (2001, 1 datum), and Qian et al. (2011, 5 data) (Figure 1). The Paperniek et al. (2011) data were approximately split between used and new tarp samples. The compiled data included 13 low density PE tarps (LDPE) and 24 high density PE tarps (HDPE). There was no significant effect of tarp history on MTC (2-way analysis of variance, new versus used, p=0.8), but the effect of material type was significant (p = 0.002). The median chloropicrin HDPE MTC of 0.82 cm h^{-1} was used here to represent PE tarps generally because LDPE tarps are rarely, if ever, used in California. This PE MTC corresponds to an equivalent boundary layer depth in HYDRUS of 330 cm.

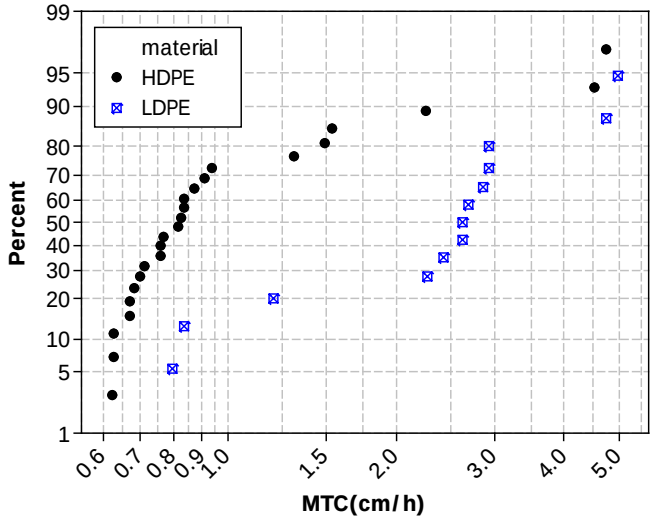

Figure 1. Cumulative frequency of HDPE and LDPE mass transfer coefficients (MTC) compiled from the literature.

Soil surface temperature Several chloropicrin transport processes are temperature dependent. HYDRUS typically requires specification of soil surface temperature as a boundary condition to simulate heat transport. Air temperature data are usually available for most field studies, but soil surface temperatures are not generally equal to air temperature, even for bare soil. When a tarp is present, under-tarp surface temperature depends on the tarp material. In the Lost Hills study, under-tarp temperatures for TIF were measured directly (Appendix 1) and these were used in the simulations here. For the bare ground and PE simulations here, a sine wave temperature model was used to generate soil surface temperatures (Šimunek et al., 2012).

[1] $$T(t) = \overline{T} + \Delta T \sin(\pi(2t - \frac{7}{12}))$$

where t is time (d), $\overline{T}$ is the average surface temperature (˚C), and ΔT is the amplitude of the daily fluctuation (˚C). For both PE and the bare surface, a simple relationship between daily soil surface and air temperature extremes was assumed.

[2] $$T_{max,i} = T_{max,air} + \delta_{max,i}$$

[3] $$T_{min,i} = T_{min,air} + \delta_{min,i}$$

where i refers to PE or bare ground, and δ_{max} and δ_{min} are the difference between daily maximum soil surface and maximum air temperatures (˚C), and difference between minimum daily soil surface and minimum air temperatures (˚C), respectively. Estimates for the bare ground δs were taken as the mean differences between calibrated soil surface temperatures (Spurlock, 2011) and measured air temperatures from nearby California Irrigation Management Information System weather stations for 3 bare ground fumigation studies conducted in Salinas, CA, and Madera and Imperial Counties, CA (Figure 2, Table 2). PE tarp δs used here were those reported by Yates et al. (1996) (Table 2).

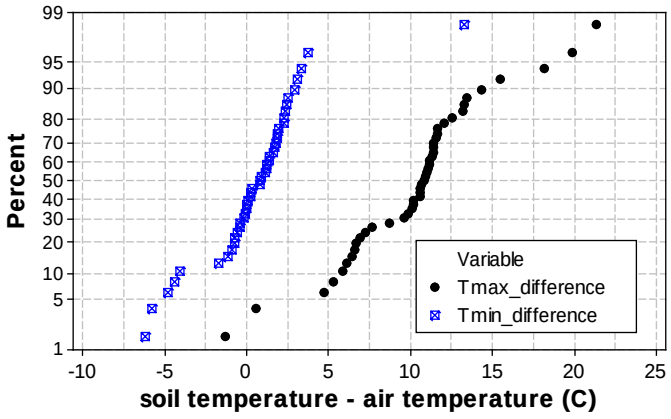

Figure 2. Cumulative frequency of differences between daily calibrated soil surface temperature extremes and nearby CIMIS weather stations temperature extremes for Salinas, Madera and Imperial County fumigation studies (Spurlock, 2011).

Table 2. Estimated differential in daily maximum and minimum temperature between soil surface and air (˚C +/- stnd dev.)

surface	$\delta_{max,i}$	$\delta_{min,i}$
i = bare ground	10.8 (+/- 4.2)	0.8 (+/- 3.0)
i =PE tarp	17.6 (+/- 3.9)	3.2 (+/- 0.8)

Equation [1] was then used to simulate surface temperatures for *i* = bare ground and *i* =PE application scenarios where

[4] $$\Delta T = (\overline{T}_{\max\_air,LostHills} + \delta_{\max,i}) - (\overline{T}_{\min\_air,LostHills} + \delta_{\min,i})$$

[5] $$\overline{T} = \frac{1}{2}\left[(\overline{T}_{\max\_air,LostHills} + \delta_{\max,i}) + (\overline{T}_{\min\_air,LostHills} + \delta_{\min,i}) \right]$$

and $\overline{T}_{\max\_air,LostHills}$ and $\overline{T}_{\min\_air,LostHills}$ are the overall mean maximum (29.7 ˚C) and mean minimum air temperatures (14.4 ˚C) over the 18 day Lost Hills field 1 study period (6/4/2011 to 6/22/2011), respectively.

Modeling domains, tarping and model outputs Figure 3 illustrates the initial chloropicrin concentration distribution, tarp locations and dimensions of the full-field broadcast (Figure 3a) and strip application (Figure 3b) modeling domains. Bare ground full-field and strip applications were identical to Figures 3a and 3b, respectively, but with no tarp. The horizontal domain length of 366 cm corresponds to the width of a single pass in typical field fumigation with tarp. For shallow scenarios depth of injection was 30 cm; for deep scenarios the depth of injection was 45 cm. Domain depth was 150 cm; in preliminary testing flux density and cumulative flux were essentially independent of domain depths > 100 cm.

In all cases applications were assumed to occur at 09:15. Simulations in the "depth of application" and "strip versus full field" comparisons were conducted for 18.3 days at which time volatilization was assumed essentially complete. The bare ground broadcast irrigation treatment simulations were conducted for 14 days. Management practice comparisons were based on cumulative flux expressed as "emission rating" (ER = volatilized fumigant/total applied) and on maximum 6 h pre-tarpcut period mean flux density (ug $m^{-2}sec^{-1}$) on a 100 lb $acre^{-1}$ (112 kg ha^{-1}) basis. The 6 h flux averaging periods were 00:00 – 06:00, 06:00-12:00, 12:00 – 18:00, and 18:00 – 24:00 such as would be used in a typical field monitoring study. For all tarped applications, the tarp holding period of 10 days was assumed, after which complete tarp removal was simulated.

The potential evaporative water flux was set to zero for the tarped portion of each modeling domain, while daily potential evaporation of 0.6 cm was used for the untarped portion of the soil

surfaces. This potential evaporation is approximately equal to early summer reference evapotranspiration rates in the San Joaquin Valley, and was simulated during daylight hours. A matric potential of -15000cm was used as the limiting soil surface pressure head at below which actual evaporation is less than potential evaporation (i.e. stage II, commonly called "soil-limited" evaporation). The lower water flow boundary condition was a "free drainage" (unit gradient) boundary condition.

End of simulation fumigant mass balances expressed as a percentage of fumigant applied were generally much less than 1% (i.e. 0.01% - 0.1%) indicating very low numerical error. The exception was for simulations of deep (45 cm) applications where sharp discontinuities in soil organic carbon between 20–40 cm and 40-60cm soil layers resulted in numerical errors of between 1 and 1.5% of application.

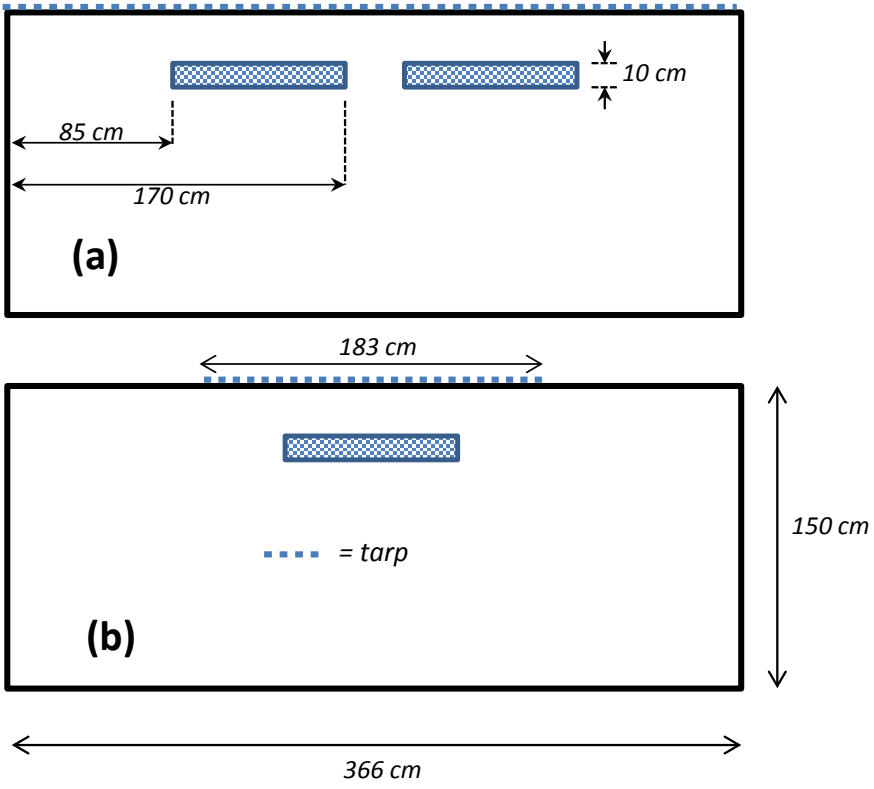

Figure 3. Modeling domain for (a) "full field" broadcast application, and (b) strip application where only 50% of field surface is covered by a tarp.

RESULTS

Depth of Application

Six simulations were conducted to compare the relative effect of 30 cm (12 inch) and 45 cm (18 inch) application depth (Table 3) under bare ground, PE and TIF tarp scenarios. One additional

simulation (simulation #3, Table 3) was conducted to illustrate the interaction of depth and soil-water content. Lost Hills field 1 soil bulk density, soil organic carbon content, and calibrated values of the chloropicrin first order degradation constant and soil sorption coefficient were used in all simulations (Table 1). Mean measured Lost Hills field 1 initial soil-water contents are used in the "normal" simulations where available water capacity (AWC) for the 0-20 cm depth was 47% (θ = 0.172 cm^3 cm^{-3}) and AWC is 72% (θ = 0.216 cm^3 cm^{-3}) for the 20-40 cm soil depth. The "dry" simulations assumed the measured 0-20 cm depth water content of 0.172 cm^3 cm^{-3} throughout the *entire* soil profile. AWC calculated from fitted field 1 van Genuchten soil hydraulic parameters (Appendix 1) as $[(\theta_i - WP)/(FC - WP)] \times 100$, where θ_i = initial water content, FC = field capacity = 0.3 bar soil water content, and WP = permanent wilting point = 15 bar soil water content. .

Table 3. Test of application depth simulation scenarios and results. All scenarios are full-field applications (no strip applications). Maximum 6 h flux density expressed on a 100 lb $acre^{-1}$ applied basis.

simulation	tarp type	application depth (cm)	water content[A]	maximum 6 h flux density (ug m^{-2} sec^{-1})	emission rating
1	bare soil	30	normal	16.4	0.31
2	bare soil	45	normal	5.4	0.16
3	bare soil	45	dry	8.2	0.20
4	PE	30	normal	6.5	0.15
5	PE	45	normal	2.5	0.08
6	TIF	30	normal	2.3	0.06
7	TIF	45	normal	0.9	0.03

[A] see text

Increasing injection depth from 30 cm to 45 cm decreased both peak 6 h flux density and emission rating in all 3 cases under the simulation scenarios here (Table 3). However, it is evident that the magnitude of the decrease is strongly dependent on initial soil-water content (Figure 4, Table 4). The influence of soil moisture is probably greatest over the 0 to ~ 50 cm depth of soil since this is the region that includes the application zone. Current labels only specify pre-application soil moisture content at the 9 inch depth (23 cm). The percentage change in ER was essentially constant across tarp type, but percent decrease in maximum flux varied with surface tarping with TIF < PE < bare ground.

This effect was largely attributable to "leakage" immediately around the tarp edge in the strip scenario as compared to a corresponding full application scenario; that leakage was greatest for the low permeability TIF tarp (Figure 6). The same effect (high fluxes immediately at edge-of-tarp) was noted by Gao et al. (2013) in dynamic flux chamber measurements during the Lost Hills study.

Table 7. Emission ratings (ER) for strip applications as compared to full field applications under bare ground, PE and TIF conditions. The "low AWC" cases correspond to Lost Hills field 1 initial water contents, while "high AWC" are Lost Hills field 3 conditions. Percent difference is [(strip ER – full ER)/full ER] * 100.

surface	soil moisture	application	ER	percent difference
BARE	low AWC	strip	0.33	6%
		full	0.32	
	high AWC	strip	0.22	9%
		full	0.21	
PE	low AWC	strip	0.20	52%
		full	0.13	
	high AWC	strip	0.15	9%
		full	0.14	
TIF	low AWC	strip	0.09	66%
		full	0.05	
	high AWC	strip	0.06	44%
		full	0.04	

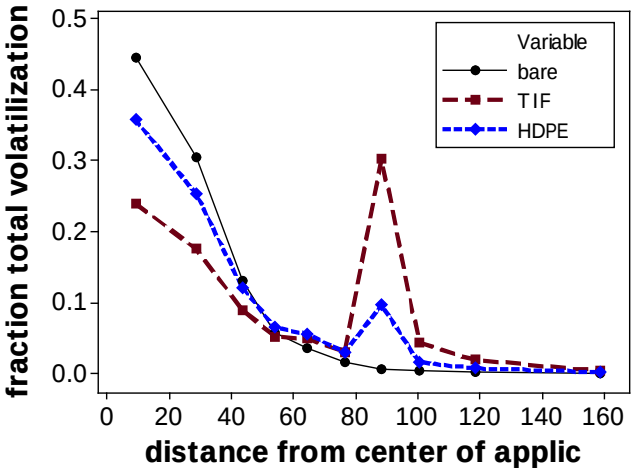

Figure 6. Relative volatilization (fraction of total within scenario) versus distance from application center (cm) for bare ground, PE and TIF scenarios. Tarp edge for PE and TIF was ≈ 90 cm from center of application. Edge of shank wing was ≈ 50 cm from center of application.

Maximum 6 h flux densities were calculated on a 100 lb ac^{-1} applied/gross field acreage basis, so the simulated total applied mass for each modeling domain (strip versus full field) was identical. The maximum flux densities were ordered similarly as the ER, with bare ground > PE > TIF. In all cases the strip applications displayed larger 6 h maximum mean flux density than the full field, However, the absolute differences between strip and full field maximum flux densities were < 2 ug m^{-2} s^{-1} in cases except for the bare ground low AWC scenario.

Table 8. Maximum 6 h flux density (ug m^{-2} s^{-1}, 100 lb/gross field acre applied basis) for strip applications as compared to full field applications under bare ground, PE and TIF conditions. The "low AWC" cases correspond to Lost Hills field 1 initial water contents, while "high AWC" are the wetter Lost Hills field 3 conditions. Percent difference is [(strip max flux– full max flux)/full max flux] * 100.

surface	soil moisture	application	maximum 6 h flux density (ug m^{-2} s^{-1})	percent difference
BARE	low AWC	strip	18.5	13%
		full	16.4	
	high AWC	strip	10.7	28%
		full	8.4	
PE	low AWC	strip	7.5	28%
		full	5.8	
	high AWC	strip	4.7	14%
		full	4.1	
TIF	low AWC	strip	4.0	73%
		full	2.3	
	high AWC	strip	3.0	49%
		full	2.0	

CONCLUSION

The effects of application depth (Tables 3 and 4), post-application irrigations (Table 5) and strip versus whole field application (Tables 7 and 8) on emission rating and maximum 6 h flux density were estimated using HYDRUS2D/3D. Insofar as possible, the simulations were conducted using soil data from the Lost Hills study. The modeling results represent relative differences in flux rating and maximum 6 h flux among management regimes for the specific conditions simulated.

The modeling results indicate that the actual effect of a particular management practice in the field will depend on several specific site factors. For example, the simulated effect of strip versus

full-field application on maximum 6 h flux varied substantially with both initial water content and tarp type (Table 8). Several other soil and site variables are known to strongly affect simulated flux (Spurlock et al., 2013b), including soil saturated water content (i.e. soil bulk density) and surface temperature.

In the simulation comparisons, a single application parameter such as depth is changed while all other conditions are identical. The effect of depth is then determined by comparing the two simulations. However, in reality there is often wide variability in soil properties *among fields*, even when soil texture and pre-fumigation preparation (tillage and irrigation) are similar (Figure 7). Thus, the simulated effects are theoretical because the modeling analysis does not account for field-to-field variability. Ideally, this variability could be represented in modeling results using stochastic modeling procedures such as Monte Carlo simulation. In particular, if we had a database of measured pre-fumigation soil data (e.g. bulk density, initial water contents) from many fields, the HYDRUS 2D/3D model could be run for each of these fields, thereby accounting, at least partially, for field-to-field variability. Unfortunately, those field to field data are not available. We are currently developing studies to obtain such data to enhance our modeling capabilities.

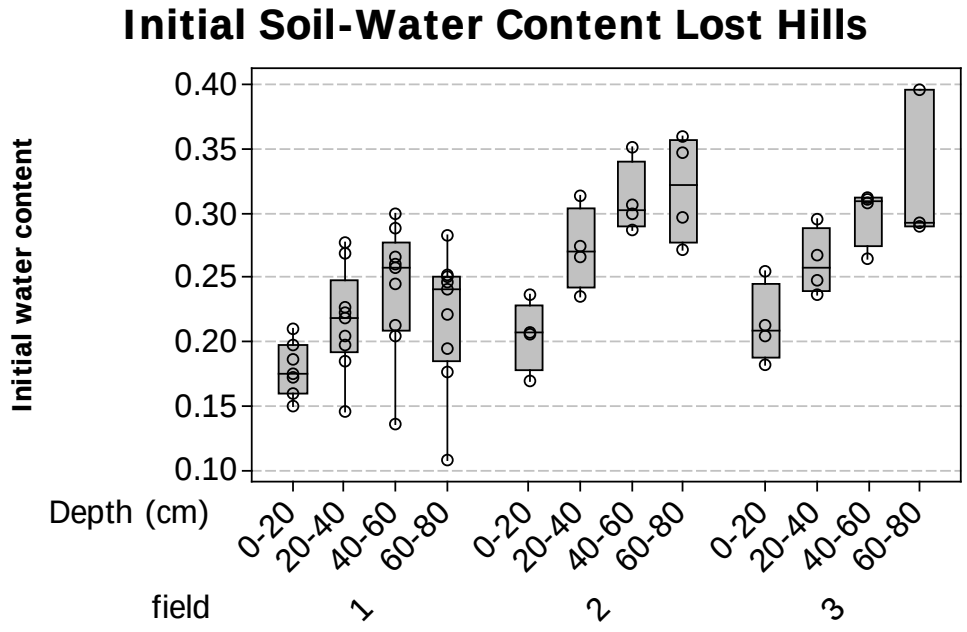

Figure 7. Lost Hills fields 1 – 3 initial soil water contents (field 1, n=9, fields 2 and 3, n=4). All soils are classified as sandy loam; pre-application irrigation and soil-cultivation were similar in all 3 fields.

It is likely that some of the modeled effects on flux, such as effect of depth, will not be evident in direct analysis of field monitoring studies. One reason is that soil hydraulic properties, soil-water contents and temperature conditions all vary among field experiments. Consequently, effects on flux due to changes in an individual parameter may not be apparent in field monitoring data unless the effects are very large (i.e. effect of tarp: TIF versus PE). Instead, differences between fields reflect the aggregate effect of several variables. A second reason why modeled effects may not manifest in field data is the intrinsic uncertainty in field-based back-calculated flux estimates (Johnson and Spurlock, 2013).

In summary, the greatest modeled flux differences between applications were attributable to differences in tarping, where ER and maximum 6 h flux densities under TIF were approximately 35 – 40 % of those in PE, while ER and maximum flux in PE were 40 – 50% of those in bare ground simulations (Tables 3 and 4). Under the conditions simulated here, increasing injection depth from 30 cm to 45 cm yielded decreases in ER and maximum 6 h flux density that were nearly as large as differences between tarps (i.e. decreases of up to ~ 50%), but that effect is dependent on initial soil-water content (Tables 3 and 4), and probably will depend on other site/soil factors. Post-application irrigations in bare ground applications yielded only modest decreases (≤ 20%) in both ER and maximum flux (Table 5). Finally, the effect of strip versus full-field application depended on both tarp-type and soil-water content in a complicated way (Tables 7 and 8). Generally speaking, the differences in ER and maximum 6 h flux were highest under tarped dry soil conditions, where fumigant could rapidly diffuse past the tarp edge and volatilize unimpeded by the tarp. The maximum 6 h flux densities were expressed on a 100 lb applied /gross field acre basis, so the results do not reflect the actual reduction in application rate that would be realized in a strip application. Maximum flux densities were always greater for strip versus full-field application, although the percent differences were small (< 30%) in the bare ground and PE cases (Table 8).

bcc: Spurlock Surname File

REFERENCES

Ajwa, H; D.A. Sullivan. 2012. Soil Fumigant Emissions Reduction using EVAL barrier resin film (VaporSafe™) and Evaluation of Tarping Duration Needed to Minimize Fumigant Total Mass Loss. Study ID HA2011A submitted to DPR, 404 pp.

Gao, S., H. Ajwa, R. Qin, M. Stanghellinin and D. Sullivan. 2013. Emission and Transport of 1,3-Dichloropropene and Chloropicrin in a Large Field Tarped with VaporSafe TIF. Environ. Sci. Technol. 47: 405−411.

Hornberger, G.M. and R.C. Spear, 1981. An Approach to the Preliminary Analysis of Environmental Systems, J. of Environ. Management 12:7–18.

Johnson, B. and F. Spurlock. 2013. Stochastic Evaluation of Back Calculation Procedures for Estimating Flux Using Data From the Lost Hills Study. DPR EM Branch memorandum. Available at: <http://www.cdpr.ca.gov/docs/emon/pubs/ehapreps/analysis_memos/2415_segawa.pdf >.

Papiernek, S.K., Yates, S.R., Chellimi, D.O. 2011. A Standardized Approach for Estimating the Permeability of Plastic Films to Soil Fumigants under Various Field and Environmental Conditions. J. Environ. Qual. 40: 1375-1382.

Papiernik, S, S.R. Yates and J. Gan. 2001. An Approach for Estimating the Permeability of Agricultural Films. Environ. Sci. Technol. 35:1240-1246.

Qian,Y., Kamel, A., Stafford, C., Nguyen, T., Chism, W.J., Dawson, J., and C. W. Smith. 2011. Evaluation of the Permeability of Agricultural Films to Various Fumigants. Environ. Sci.Technol. Environ. Sci. Technol. 45:9711–9718.

Šimunek, J., M. Th. van Genuchten, and M. Šejna. 2012. The HYDRUS Software Package for Simulating Two- and Three-Dimensional Movement of Water, Heat, and Multiple Solutes in Variably-Saturated Media, Technical Manual, Version 2.0, PC Progress, Prague, Czech Republic, pp. 260.

Spurlock, F. 2011. Simulation of Three Untarped 1,3-Dichloropropene Flux Studies Using HYDRUS. DPR EM Branch memorandum. Available at: <http://www.cdpr.ca.gov/docs/emon/pubs/ehapreps/analysis_memos/2277_segawa.pdf >.

Spurlock, F., B. Johnson and A. Tuli. 2013a. HYDRUS Simulation of Chloropicrin and 1,3-Dichloropropene Transport and Volatilization in the Lost Hills Fumigation Trials. DPR EM Branch memorandum. Available at: <http://www.cdpr.ca.gov/docs/emon/pubs/ehapreps/analysis_memos/2420-segawa_final.pdf >.

Spurlock,F., J. Šimůnek, B. Johnson, and A. Tuli. 2013b. Sensitivity Analysis of Soil Fumigant Transport and Volatilization to the Atmosphere. Vadose Zone Journal. doi:10.2136/vzj2012.0130

van Genuchten, M. Th. 1980. A Closed-form Equation for Predicting the Hydraulic Conductivity of Unsaturated Soils. Soil Sci. Soc. Am. J., 44:892-898.

Yates, S.R., J. Gan, F.F. Ernst, A. Mutziger, and M.V. Yates. 1996. Methyl bromide emissions from a covered field: I. Experimental conditions and degradation in soil. J. Environ. Qual. 25:184-192.

Appendix 1

Table A-1. Mean initial soil water content for fields 1 and 3 in Lost Hills.

Field 1 (N=9)		
layer (cm)	**mean theta_initial**	**SDeviation**
0-20	**0.172**	**0.022**
20-40	**0.216**	**0.041**
40-60	**0.241**	**0.050**
60-80	**0.219**	**0.053**
Field 3 (N=4)		
layer	**mean theta_initial**	**SDeviation**
0-20	**0.213**	**0.031**
20-40	**0.262**	**0.026**
40-60	**0.299**	**0.023**
60-80	**0.313**	**0.056**

Appendix 1

Table A-2. Soil data used in HYDRUS simulations. Soil properties between 80 and 150 cm were assumed identical to layer 4 (60 – 80 cm) properties. Hydraulic parameters fit using data in Table A-1.

Input Variable (units)	Variable name	Layer 1 0-20cm	Layer 2 20-40 cm	Layer 3 40-60 cm	Layer 4 60-80 cm
Field 1					
ρ_b ($cm^3 g^{-1}$)	soil bulk density	1.474	1.189	1.527	1.381
θ_s (-)	saturated water content	0.545	0.445	0.442	0.446
θ_i (-)	initial water content	0.172	0.216	0.241	0.219
θ_r (-)	residual water content	0.039	0.039	0.039	0.039
α (cm^{-1})	VG retention model parameter	0.15796	0.057833	0.04505	0.05552
n (-)	VG retention model parameter	1.2427	1.22544	1.19846	1.2108
OC (g OC g^{-1})	soil organic carbon	0.60	0.50	0.00	0.00
Field 3					
ρ_b $cm^3 g^{-1}$	soil bulk density	1.288	1.464	1.51	1.379
θ_s (-)	saturated water content	0.514	0.4475	0.430	0.483
θ_i (-)	initial water content	0.213	0.262	0.299	0.313
θ_r (-)	residual water content	0.039	0.039	0.039	0.039
α (cm^{-1})	VG retention model parameter	0.265982	0.144417	0.114204	0.04287
n (-)	VG retention model parameter	1.19079	1.14313	1.15657	1.19182
OC (g OC g^{-1})	soil organic carbon	0.59	0.45	0.21	0.17

Appendix 1

Table A-3. Principal input variables required for HYDRUS simulations.

Input Variable (units)	Variable name	Source
ρ_b (cm^3(gm soil)$^{-1}$)	soil bulk density[A]	measured
θ_s (-)	saturated water content[A]	calculated from bulk density ($\theta_s = 1 - \rho_b/2.65$)
θ_i (-)	initial water content[A]	measured
θ_r (-)	residual water content[A]	sandy loam texture class mean (Carsel and Parrish, 1988)
α (cm^{-1})	VG retention model parameter[A, B]	measured
n (-)	VG retention model parameter[A, B]	measured
K_s (cm d^{-1})	saturated hydraulic conductivity[A]	sandy loam texture class mean (Carsel and Parrish, 1988)
C_n (J cm^3 K^{-1})	volumetric solid phase heat capacity[A]	HYDRUS default
λ_L, b_1, b_2, b_3	soil thermal conductivity parameters[A]	Chung and Horton (1980)
$T_0(t)$ (C)	soil surface temperature as function of time *t*	measured – surrogate field plot
D_g (cm^2 d^{-1})	gas phase diffusion coefficient	SPARC on-line calculator (Hilal et al., 2003a, 2003b)
D_gE_a (J mol^{-1})	D_g activation energy[C]	SPARC on-line calculator (Hilal et al., 2003a, 2003b)
D_w (cm^2 d^{-1})	aqueous phase diffusion coefficient	SPARC on-line calculator (Hilal et al., 2003a, 2003b)
D_wE_a (J mol^{-1})	D_w activation energy[C]	SPARC on-line calculator (Hilal et al., 2003a, 2003b)
K_h (-)	Henry's law constant	*chloropicrin:* Kawamoto and Urano (1989)
K_hE_a (J mol^{-1})	K_h activation energy[C]	*chloropicrin:* Chikos and Acree (2006)
k_1 (d^{-1})	first-order degradation rate constant[A]	**calibrated**
k_1E_a (J mol^{-1})	k_1 activation energy[A,C]	mean [data of Dungan et al. (2003) and Gan et al. (2000)]
OC (g OC (g $soil^{-1}$)	soil organic carbon mass fraction[A]	measured
K_d (ml^3 g^{-1})	soil partition coefficient[A]	calculated from **calibrated** K_{OC} and measured OC ($K_d = K_{OC}$ * OC)
d (cm)	tarp boundary layer depth[D]	**calibrated**
λ_w (cm)	longitudinal dispersivity	HYDRUS default

[A] required for each soil layer

[B] van Genuchten (VG) soil-water retention model was used (van Genuchten, 1980)

[C] activation energies describe the temperature dependence of the associated parameter (Spurlock et al., 2012)

[D] tarp boundary layer depth (describes tarp permeability) assumed independent of temperature – see calibration discussion.

Appendix 1

Table A-4. Chemical and tarp property input variables used for HYDRUS simulations.

Input Variable (units)	Variable name	Source
D_g (cm^2 d^{-1})	gas diffusion coefficient *chloropicrin:* 6515	SPARC on-line calculator (Hilal et al., 2003a, 2003b)
D_gE_a (J mol^{-1})	D_g activation energy *chloropicrin:* 4566	SPARC on-line calculator (Hilal et al., 2003a, 2003b)
D_w (cm^2 d^{-1})	aq. diffusion coefficient *chloropicrin:* 0.707	SPARC on-line calculator (Hilal et al., 2003a, 2003b)
D_wE_a (J mol^{-1})	D_w activation energy *chloropicrin:* 17920	SPARC on-line calculator (Hilal et al., 2003a, 2003b)
K_h (-)	Henry's constant. *chloropicrin:* 0.083	*chloropicrin:* Kawamoto and Urano (1989);
K_hE_a (J mol^{-1})	K_h activation energy *chloropicrin:* 39120	*chloropicrin:* Chikos and Acree (2006)
k_1 (d^{-1})	degradation constant *chloropicrin:* 0.1595	**calibrated from field 1 data**
k_1E_a (J mol^{-1})	k_1 activation energy *chloropicrin:* 56933	mean [data of Dungan et al. (2003) and Gan et al. (2000)]
K_{OC} ml (g OC)$^{-1}$	OC-normalized soil partition coefficient. *chloropicrin:* 66	**calibrated from field 1 data**
d (cm)	TIF boundary layer depth (tarp permeability) *chloropicrin:* 2230	**calibrated from field 1 data**

Appendix 1

Figure A-1. Lost Hills undertarp temperature (TIF tarp, 6/4/2011 – 6/20/2011).